Neutron spin resonance as a probe of superconducting gap anisotropy in partially detwinned electron underdoped $NaFe_{0.985}Co_{0.015}As$

Chenglin Zhang,[1] J. T. Park,[2] Xingye Lu,[1,3] Rong Yu,[4,5] Yu Li,[1] Wenliang Zhang,[3] Yang Zhao,[6,7] J. W. Lynn,[6] Qimiao Si,[1] and Pengcheng Dai[1,*]

[1]*Department of Physics and Astronomy, Rice University, Houston, Texas 77005, USA*
[2]*Heinz Maier-Leibnitz Zentrum, Technische Universität München, D-85748 Garching, Germany*
[3]*Institute of Physics, Chinese Academy of Sciences, Beijing 100190, China*
[4]*Department of Physics and Beijing Key Laboratory of Opto-electronic Functional Materials and Micro-nano Devices, Renmin University of China, Beijing 100872, China*
[5]*Department of Physics and Astronomy, Collaborative Innovation Center of Advanced Microstructures, Shanghai Jiaotong University, Shanghai 200240, China*
[6]*NIST Center for Neutron Research, National Institute of Standards and Technology, Gaithersburg, Maryland 20899-6102, USA*
[7]*Department of Materials Science and Engineering, University of Maryland, College Park, Maryland 20742, USA*

(Received 3 February 2015; revised manuscript received 12 March 2015; published 27 March 2015)

We use inelastic neutron scattering (INS) to study the spin excitations in partially detwinned $NaFe_{0.985}Co_{0.015}As$ which has coexisting static antiferromagnetic (AF) order and superconductivity ($T_c = 15$ K, $T_N = 30$ K). In previous INS work on a twinned sample, spin excitations formed a dispersive sharp resonance near $E_{r1} = 3.25$ meV and a broad dispersionless mode at $E_{r1} = 6$ meV at the AF ordering wave vector $\mathbf{Q}_{AF} = \mathbf{Q}_1 = (1,0)$ and its twinned domain $\mathbf{Q}_2 = (0,1)$. For partially detwinned $NaFe_{0.985}Co_{0.015}As$ with the static AF order mostly occurring at $\mathbf{Q}_{AF} = (1,0)$, we still find a double resonance at both wave vectors with similar intensity. Since $\mathbf{Q}_1 = (1,0)$ characterizes the explicit breaking of the spin rotational symmetry associated with the AF order, these results indicate that the double resonance cannot be due to the static and fluctuating AF orders but originate from the superconducting gap anisotropy.

DOI: 10.1103/PhysRevB.91.104520 PACS number(s): 74.25.Ha, 74.70.−b, 78.70.Nx

I. INTRODUCTION

The neutron spin resonance is a collective magnetic excitation observed by inelastic neutron scattering (INS) at the antiferromagnetic (AF) ordering wave vector of unconventional superconductors below T_c [1–4]. First discovered in the optimally hole-doped $YBa_2Cu_3O_{6+x}$ family of copper oxide superconductors [1], the mode was also found in iron pnictide superconductors at the AF wave vector $\mathbf{Q}_{AF} = (1,0)$ in reciprocal space [Figs. 1(a) and 1(b)] [5–16] and is considered one of the hallmarks of unconventional superconductivity [17]. Experimentally, the neutron spin resonance appears as an enhancement of the magnetic spectral weight at an energy E_r in the superconducting state at the expense of normal-state spin excitations for energies below it. For iron pnictide superconductors with hole and electron Fermi surfaces near the Γ and M points, respectively [Fig. 1(c)] [18,19], the mode is generally believed to arise from sign-reversed quasiparticle excitations between the hole and electron Fermi surfaces and to occur at an energy below the sum of their superconducting gap energies ($E_r \leqslant \Delta_h + \Delta_e$) [20,21].

If the energy of the resonance is associated with the superconducting gap energies at the hole and electron Fermi surfaces, it should be sensitive to their anisotropy on the respective Fermi surfaces [22,23]. Indeed, recent INS experiments on the $NaFe_{1-x}Co_xAs$ family of iron pnictide superconductors reveal the presence of a dispersive sharp resonance near $E_{r1} = 3.25$ meV and a broad dispersionless mode at $E_{r2} = 6$ meV at $\mathbf{Q}_{AF} = (1,0)$ in electron underdoped superconducting $NaFe_{0.985}Co_{0.015}As$ with static AF order ($T_c = 15$ K and $T_N = 30$ K) [15,16]. From the electronic phase diagram of $NaFe_{1-x}Co_xAs$ determined from specific heat [24], scanning tunneling microscopy [25], and nuclear magnetic resonance (NMR) [26,27] experiments, we know that $NaFe_{0.985}Co_{0.015}As$ is a bulk superconductor with microscopically coexisting static AF-ordered and superconducting phases. For Co doping near optimal superconductivity around $x = 0.0175$, $NaFe_{1-x}Co_xAs$ becomes mesoscopically phase separated with static AF-ordered and paramagnetic superconducting phases [27], similar to the coexisting cluster spin-glass and superconducting phases in optimally electron-doped $BaFe_2As_2$ [28,29]. Since angle-resolved photoemission spectroscopy (ARPES) experiments on $NaFe_{0.985}Co_{0.015}As$ found a large superconducting gap anisotropy in the electron Fermi pockets [30], the double resonance may result from orbital-selective pairing-induced superconducting gap anisotropy along the electron Fermi surfaces [31]. Upon increasing electron doping to $x = 0.045$ to form superconducting $NaFe_{0.955}Co_{0.045}As$ ($T_c = 18$ K), the superconducting gap anisotropy disappears [32,33], and INS reveals only a single sharp resonance coupled with superconductivity [34].

Although the superconducting gap anisotropy provided a possible interpretation [31], the double resonance in underdoped $NaFe_{0.985}Co_{0.015}As$ may also be due to the coexisting static AF order with superconductivity [35,36]. Since $\mathbf{Q}_{AF} = \mathbf{Q}_1 = (1,0)$ characterizes the explicit breaking of the spin rotational symmetry in the AF-ordered state of a completely detwinned sample [Figs. 1(b) and 1(c)] [37], one should expect magnetic susceptibility anisotropy at $\mathbf{Q}_{AF} = \mathbf{Q}_1 = (1,0)$ and $\mathbf{Q}_2 = (0,1)$. At the AF-ordering wave vector $\mathbf{Q}_{AF}$=$\mathbf{Q}_1$=(1,0),

*pdai@rice.edu

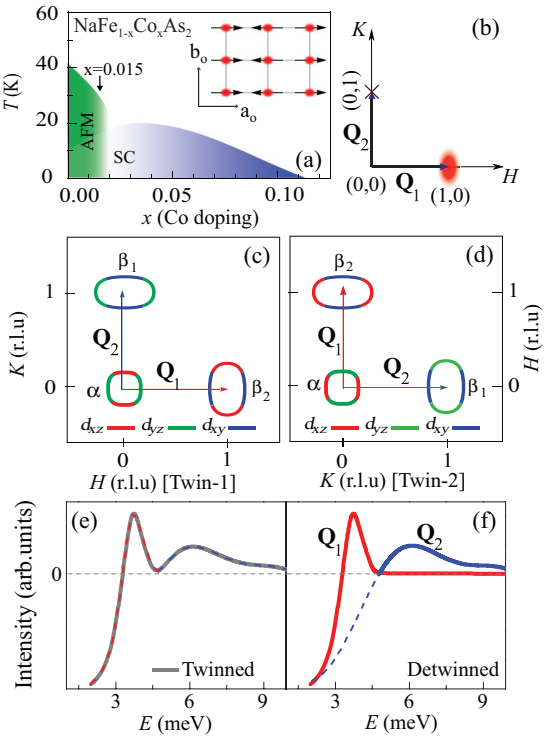

FIG. 1. (Color online) (a) The electronic phase diagram of $NaFe_{1-x}Co_xAs$, where the arrow indicates the Co-doping level of our sample. The inset shows the magnetic structure in orthorhombic notation. (b) In a 100% detwinned sample, one should observe magnetic order at $\mathbf{Q}_{AF} = \mathbf{Q}_1 = (1,0)$ but not at $\mathbf{Q}_2 = (0,1)$. (c) The schematic drawings of the Fermi surfaces in a detwinned sample. (d) Its twin domain rotated 90° away. The arrows mark Fermi surface nesting wave vectors. (e) In a twinned sample, one cannot distinguish $\mathbf{Q}_1 = (1,0)$ and $\mathbf{Q}_2 = (0,1)$, and therefore there should be two resonances at both wave vectors. (f) In the AF order and superconductivity coexisting theory, E_{r1} should appear at $\mathbf{Q}_1$ and E_{r2} at $\mathbf{Q}_2$ in a completely detwinned superconducting sample with static AF order at $\mathbf{Q}_1$.

the resonance appears in the longitudinal susceptibility, whereas the transverse component displays a spin-wave Goldstone mode. At the other momentum $\mathbf{Q}_2 = (0,1)$, the resonance has both longitudinal and transverse components and is isotropic in space. If the resonance shows distinct energy scales at $\mathbf{Q}_1$ and $\mathbf{Q}_2$, one would expect to find a double resonance in a twinned sample, as shown in Fig. 1(e) [35,36]. However, one would then expect a single resonance of energy E_{r1} at $\mathbf{Q}_1$ and that of energy E_{r2} at $\mathbf{Q}_2$ in a completely detwinned superconducting sample with static AF order [Fig. 1(f)].

To test if this is, indeed, the case, we have carried out INS experiments on uniaxial strain partially detwinned $NaFe_{0.985}Co_{0.015}As$ to study the neutron spin resonance at $\mathbf{Q}_1$ and $\mathbf{Q}_2$. Instead of E_{r1} at $\mathbf{Q}_1$ and E_{r2} at $\mathbf{Q}_2$ as expected from the theory of coexisting static AF order with superconductivity [35,36], we find that both E_{r1} and E_{r2} are present at $\mathbf{Q}_1$ and $\mathbf{Q}_2$ as in the twinned case. Therefore, the presence of the double resonance is not directly associated with the breaking of the spin rotational symmetry in detwinned $NaFe_{0.985}Co_{0.015}As$. Instead, our results are consistent with the notion that the splitting of the resonance is due to superconducting gap anisotropy in the underdoped $NaFe_{0.985}Co_{0.015}As$, suggesting weak direct coupling between spin waves and superconductivity. These results are also consistent with polarized neutron scattering data, where the longitudinal spin excitations of E_{r1} reveal a clear order-parameter-like increase below T_c reminiscent of the resonance, while the transverse spin excitations of the E_{r1} from the spin-wave Goldstone mode have no anomaly across T_c [16].

II. EXPERIMENTAL RESULTS AND THEORETICAL CALCULATIONS

We prepared single crystals of $NaFe_{0.985}Co_{0.015}As$ by the self-flux method [15] and cut a large crystal into the rectangular shape along the [1,0,0] and [0,1,0] directions ($16.11 \times 8.41 \times 1.31$ mm^3, ~0.79 g). From NMR measurements [27], we know that the tetragonal-to-orthorhombic structural transition happens around $T_s \approx 40$ K, above T_N and T_c. Our neutron scattering experiments were carried out on the PUMA and BT-7 thermal triple-axis spectrometers at the Heinz Maier-Leibnitz Zentrum (MLZ), Technische Universität München, Germany [11], and NIST Center for Neutron Research (NCNR), Gaithersburg, Maryland [38], respectively. In both cases, we used a vertically and horizontally focused pyrolytic monochromator and analyzer with a fixed final neutron energy of $E_f = 14.7$ meV. The wave vector $\mathbf{Q}$ at (q_x,q_y,q_z) (in Å^{-1}) is defined as the $(H,K,L) = (q_x a/2\pi, q_y a/2\pi, q_z c/2\pi)$ reciprocal lattice unit using the orthorhombic unit cell ($a \approx b \approx 5.589$ Å and $c = 6.980$ Å at 3 K). In this notation, the AF Bragg peaks occur at the $(1,0,L)$ positions, with $L = 0.5, 1.5, \ldots$, and there are no magnetic peaks at $(0,1,L)$ [Figs. 1(a) and 1(b)] [39]. We have used a detwinning device similar to that of the previous INS work on $BaFe_{2-x}Ni_xAs_2$ [40]. The samples are aligned in the $[1,0,0.5] \times [0,1,0.5]$ scattering plane. In this scattering geometry, we can probe the static AF order and spin excitations at both $\mathbf{Q}_1$ and $\mathbf{Q}_2$, thus allowing a conclusive determination of the detwinning ratio and spin excitation anisotropy at these wave vectors. Figures 2(a) and 2(b) show the temperature differences in transverse elastic scans along the $[H,1-H,0.5]$ and $[H,1-H,0.5]$ directions, respectively, for $NaFe_{0.985}Co_{0.015}As$ between 2 and 41 K. By comparing the scattering intensity at these two wave vectors, we estimate that the sample is about 58% detwinned. Figure 2(c) shows the temperature dependence of the magnetic order parameters. Consistent with previous data on a twinned sample [15], the uniaxial strain used to detwin the sample does not seem to alter $T_N \approx 30$ K and $T_c = 15$ K.

In previous INS work on twinned $NaFe_{0.985}Co_{0.015}As$, superconductivity induced a dispersive sharp resonance near $E_{r1} = 3.25$ meV and a broad dispersionless mode at $E_{r2} = 6$ meV at $\mathbf{Q}_1 = (1,0,0.5)$ and $\mathbf{Q}_2 = (0,1,0.5)$ [15]. To explore what happens in the uniaxial strain detwinned $NaFe_{0.985}Co_{0.015}As$, we carried out constant-$\mathbf{Q}$ scans at wave vectors $\mathbf{Q}_2$ [Fig. 2(d)] and $\mathbf{Q}_1$ [Fig. 2(e)] below and above T_c. While it is difficult to see the resonance in the raw data, the temperature differences between 5 and 21 K plotted in Fig. 2(f) reveal a sharp peak at $E_{r1} = 3.75$ meV and a broad peak at $E_{r2} = 6$ meV, in addition to the negative scattering below 3 meV due to a spin gap. These data indicate the presence

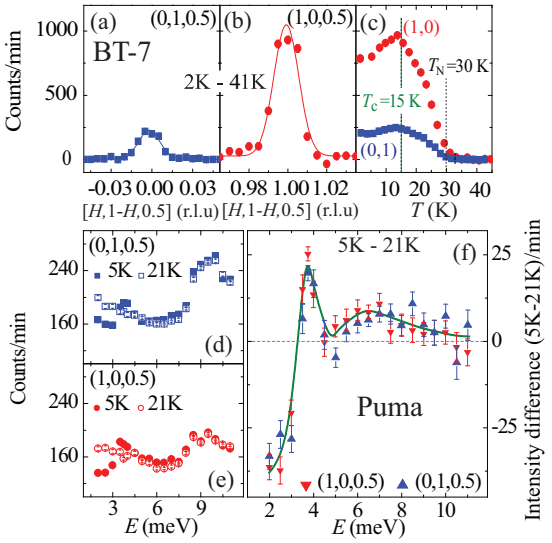

FIG. 2. (Color online) Temperature differences of the elastic scattering below (2 K) and above (41 K) the Néel temperature ($T_N = 33$ K) at reciprocal positions (a) (0,1,0.5) and (b) (1,0,0.5) in a uniaxial strained $NaFe_{0.985}Co_{0.015}As$ single crystal. The uniaxial strain along the b axis is ∼10 MPa, and data were collected on BT-7. By comparing the area ratio of the two peaks, we estimate that ∼58% ($\approx [I(1,0,0.5) - I(0,1,0.5)]/[I(1,0,0.5) + I(0,1,0.5)]$) of the crystal is detwinned. The solid lines are Gaussian fits to the data. A similar detwinning ratio is also obtained at PUMA. After releasing the uniaxial strain, we find that the sample returns to the twinned state. (c) Temperature dependence of the magnetic order parameters at $\mathbf{Q}_1$ and $\mathbf{Q}_2$ in uniaxially strained detwinned $NaFe_{0.985}Co_{0.015}As$. (d) and (e) Constant $\mathbf{Q}$ scans at $\mathbf{Q}_1$ and $\mathbf{Q}_2$ below and above T_c, respectively, in the partially detwinned sample. The peaks around ∼9 mV in the raw data are mostly temperature-independent background scattering. (f) Temperature differences between 5 and 21 K, revealing the superconductivity-induced resonance at $\mathbf{Q}_1$ and $\mathbf{Q}_2$. The nearly identical resonances at these two vectors suggest that the coupling between spin waves and superconductivity is weak in Co-doped NaFeAs. The solid line is a guide to the eye.

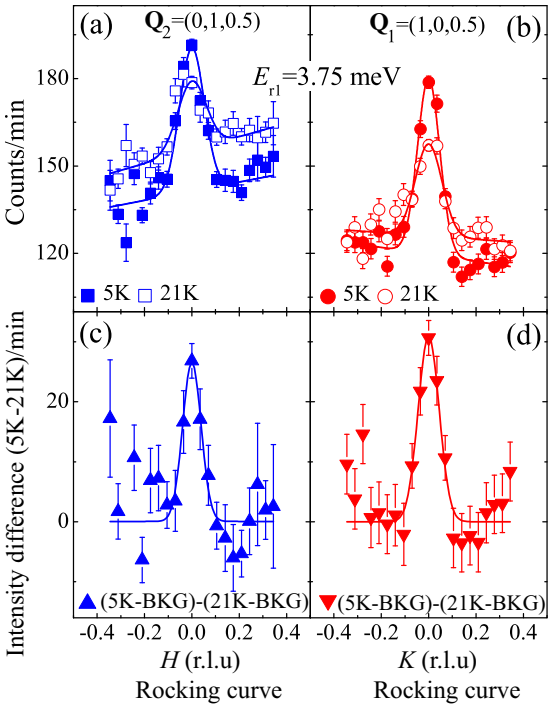

FIG. 3. (Color online) Constant-energy scans at the low-energy resonance $E_{r1} = 3.75$ meV for detwinned $NaFe_{0.985}Co_{0.015}As$. (a) and (b) The rocking scans across $\mathbf{Q}_2 = (0,1,0.5)$ and $\mathbf{Q}_1 = (1,0,0.5)$ positions above (21 K) and below (5 K) T_c, respectively. The wave-vector-independent background scattering increases slightly on warming. (c) and (d) Corresponding difference between the two temperatures after the background subtraction. The solid lines are fits to Gaussians on flat backgrounds set to zero.

of a superconductivity-induced sharp resonance and a broad resonance above a spin gap, similar to the results on twinned samples [15]. Surprisingly, there are no observable differences for the resonance at $\mathbf{Q}_1$ and $\mathbf{Q}_2$, suggesting that the double resonance is not directly associated with the twinning state of the sample.

To confirm the conclusion of Fig. 2, we carried out constant-energy scans near $\mathbf{Q}_1$ and $\mathbf{Q}_2$ at E_{r1} and E_{r2} above and below T_c. Figures 3(a) and 3(b) show transverse rocking curve scans through $\mathbf{Q}_2 = (0,1,0.5)$ and $\mathbf{Q}_1 = (1,0,0.5)$, respectively, at the sharp resonance energy $E_{r1} = 3.75$ meV above and below T_c. While there is slightly more magnetic scattering at the AF ordering wave vector $\mathbf{Q}_1 = (1,0,0.5)$ compared with that at $\mathbf{Q}_2 = (0,1,0.5)$ in both the normal and superconducting states [40], the superconductivity-induced intensity changes shown in Figs. 3(c) and 3(d), defined as the resonance [2], at these two wave vectors are indistinguishable within the statistics of our measurement.

Figures 4(a)–4(d) summarize wave-vector scans at the energy of the broad resonance $E_{r2} = 6$ meV around $\mathbf{Q}_2 = (0,1,0.5)$ and $\mathbf{Q}_1 = (1,0,0.5)$. Similar to data at $E_{r1} = 3.75$ meV, we find that the superconductivity-induced intensity gain of the broad resonance is almost indistinguishable at these wave vectors, again confirming the notion that the resonance is not sensitive to the twinning state of the system.

In electron-doped $NaFe_{1-x}Co_xAs$, the dominant orbital character of the electron pockets would be $d_{xy/xz}$ at (1,0) and $d_{yz/xy}$ at (0,1) in the Brillouin zone [Fig. 1(c)] [30,32,33]. The orbital character of the hole pocket is $d_{xz/yz}$. If the superconducting pairing amplitudes are highly orbital dependent, i.e., $\Delta_{xy} \neq \Delta_{xz/yz}$, the superconducting gap can be anisotropic along the electron pocket, and this gap anisotropy gives rise to a splitting of the resonance peak [31]. Such an orbital-selective pairing scenario is consistent with both ARPES measurements [30] and INS results in twinned samples [15].

In the uniaxial strain detwinned sample, the degeneracy of the d_{xz} and d_{yz} orbitals is lifted, and correspondingly, the Fermi surface is distorted [30]. To investigate whether the double resonances in the orbital-selective pairing scenario still exist in the presence of a splitting between the d_{xz} and d_{yz} orbitals, we calculated the imaginary part of the spin susceptibility χ'' in the superconducting state from a multiorbital $t - J_1 - J_2$ model with an orbital splitting term $\epsilon = n_{xz} - n_{yz}$ [31]. Our result for a strong orbital selectivity is presented in Fig. 5. We find two resonance peaks at each of the wave vectors $\mathbf{Q}_1$ and

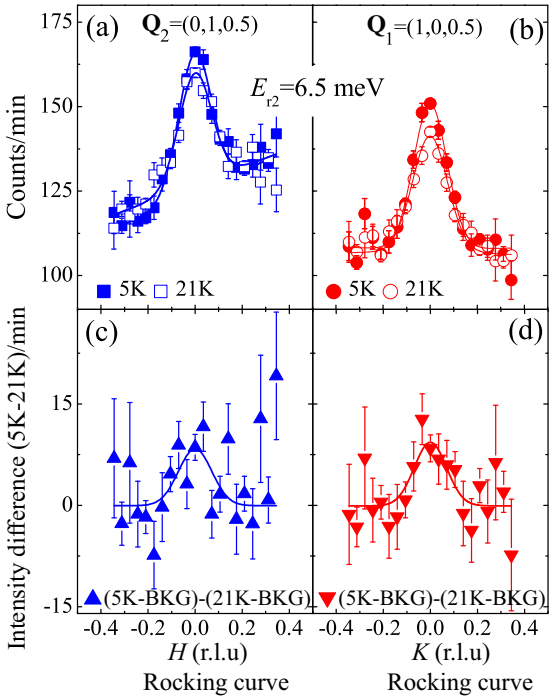

FIG. 4. (Color online) Constant-energy scans through the high-energy resonance $E_{r2} = 6.5$ meV for detwinned $NaFe_{0.985}Co_{0.015}As$. (a) and (b) The rocking scans across the $\mathbf{Q}_2 = (0,1,0.5)$ and $\mathbf{Q}_1 = (1,0,0.5)$ positions above (21 K) and below (5 K) T_c, respectively. (c) and (d) The corresponding difference between the two temperatures. The solid lines are fits to Gaussians on zero backgrounds.

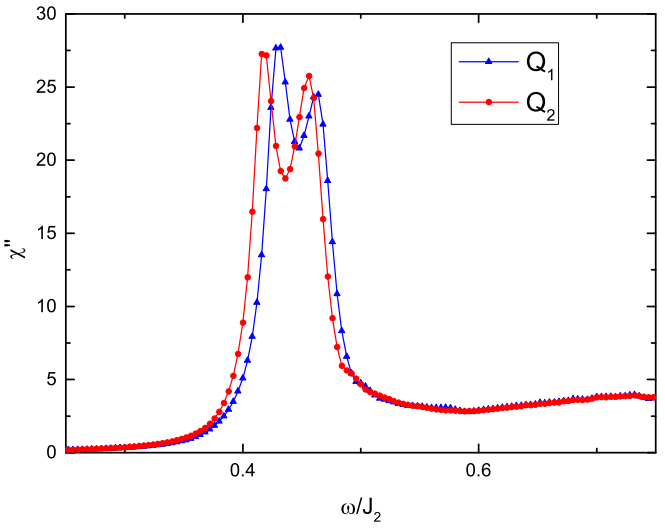

FIG. 5. (Color online) Imaginary part of the dynamic spin susceptibility χ'' in the superconducting state of a multiorbital $t - J_1 - J_2$ model with a nonzero splitting between the d_{xz} and d_{yz} orbitals, $\epsilon = 0.02$ eV. Two resonance peaks are present in each of the $\mathbf{Q}_1$ and $\mathbf{Q}_2$ wave vectors. In the calculation, $J_1/J_2 = 0.1$ is taken such that the pairing amplitudes show strong orbital selectivity. See Ref. [31] for details of the model and the method.

$\mathbf{Q}_2$ for a nonzero splitting ϵ. The intensities of the counterpart peaks at $\mathbf{Q}_1$ and $\mathbf{Q}_2$ are comparable. At each resonance peak, there is a relative shift of the resonance energy between the $\mathbf{Q}_1$ and $\mathbf{Q}_2$ resonances. This shift is proportional to the splitting ϵ. The calculated double-resonance feature at both $\mathbf{Q}_1$ and $\mathbf{Q}_2$ is qualitatively consistent with the experimental observation in the detwinned sample. The experiment cannot resolve a relative shift of the resonance energy. This could be because either the splitting ϵ is small in the detwinned underdoped compound or the coupling between the superconductivity and the splitting ϵ is rather weak. Further comparison between theory and experiments is needed to fully settle the issue.

III. CONCLUSIONS

In conclusion, our INS experiments on partially detwinned $NaFe_{0.985}Co_{0.015}As$ reveal the presence of two resonances at each of the wave vectors $\mathbf{Q}_{AF} = \mathbf{Q}_1 = (1,0)$ and $\mathbf{Q}_2$=(0,1). This is different from the scenario in which the two resonances are due to the coexisting AF order with superconductivity [35,36]. Instead, the data are qualitatively consistent with the proposal that the double resonances originate from an orbital dependence of the superconducting pairing. Our results provide further evidence that orbital selectivity plays an important role in understanding not only the normal state but also the superconducting pairing of the multiorbital electrons in the iron pnictides.

ACKNOWLEDGMENTS

We thank Z. C. Sims for his help in single-crystal growth efforts. The single-crystal growth and neutron scattering work at Rice are supported by the U.S. DOE, BES, under Contract No. DE-SC0012311 (P.D.). Part of the work is also supported by the Robert A. Welch Foundation Grants No. C-1893 (P.D.) and No. C-1411 (Q.S.). Q.S. is also supported by U.S. NSF Grant No. DMR-1309531. R.Y. was supported by NSFC Grant No. 11374361 and the Fundamental Research Funds for the Central Universities and the Research Funds of Renmin University of China.

[1] J. Rossat-Mignod, L. P. Regnault, C. Vettier, P. Bourges, P. Burlet, J. Bossy, J. Y. Henry, and G. Lapertot, Phys. C (Amsterdam, Neth.) **185**, 86 (1991).
[2] M. Eschrig, Adv. Phys. **55**, 47 (2006).
[3] J. M. Tranquada, G. Xu, and I. A. Zaliznyak, J. Magn. Magn. Mater. **350**, 148 (2014).
[4] P. C. Dai, J. P. Hu, and E. Dagotto, Nat. Phys. **8**, 709 (2012).
[5] Y. Kamihara, T. Watanabe, M. Hirano, and H. Hosono, J. Am. Chem. Soc. **130**, 3296 (2008).
[6] C. de la Cruz, Q. Huang, J. W. Lynn, J. Y. Li, W. Ratcliff II, J. L. Zarestky, H. A. Mook, G. F. Chen, J. L. Luo, N. L. Wang, and P. C. Dai, Nature (London) **453**, 899 (2008).
[7] A. D. Christianson, E. A. Goremychkin, R. Osborn, S. Rosenkranz, M. D. Lumsden, C. D. Malliakas, I. S. Todorov,

H. Claus, D. Y. Chung, M. G. Kanatzidis, R. I. Bewley, and T. Guidi, Nature (London) **456**, 930 (2008).

[8] C. Zhang, M. Liu, Y. Su, L.-P. Regnault, M. Wang, G. Tan, T. Brückel, T. Egami, and P. Dai, Phys. Rev. B **87**, 081101(R) (2013).

[9] N. Qureshi, C. H. Lee, K. Kihou, K. Schmalzl, P. Steffens, and M. Braden, Phys. Rev. B **90**, 100502(R) (2014).

[10] M. D. Lumsden, A. D. Christianson, D. Parshall, M. B. Stone, S. E. Nagler, G. J. MacDougall, H. A. Mook, K. Lokshin, T. Egami, D. L. Abernathy, E. A. Goremychkin, R. Osborn, M. A. McGuire, A. S. Sefat, R. Jin, B. C. Sales, and D. Mandrus, Phys. Rev. Lett. **102**, 107005 (2009).

[11] S. Chi, A. Schneidewind, J. Zhao, L. W. Harriger, L. J. Li, Y. K. Luo, G. H. Cao, Z. A. Xu, M. Loewenhaupt, J. P. Hu, and P. C. Dai, Phys. Rev. Lett. **102**, 107006 (2009).

[12] D. S. Inosov, J. T. Park, P. Bourges, D. L. Sun, Y. Sidis, A. Schneidewind, K. Hradil, D. Haug, C. T. Lin, B. Keimer, and V. Hinkov, Nat. Phys. **6**, 178 (2010).

[13] P. Steffens, C. H. Lee, N. Qureshi, K. Kihou, A. Iyo, H. Eisaki, and M. Braden, Phys. Rev. Lett. **110**, 137001 (2013).

[14] M. G. Kim, G. S. Tucker, D. K. Pratt, S. Ran, A. Thaler, A. D. Christianson, K. Marty, S. Calder, A. Podlesnyak, S. L. Bud'ko, P. C. Canfield, A. Kreyssig, A. I. Goldman, and R. J. McQueeney, Phys. Rev. Lett. **110**, 177002 (2013).

[15] C. L. Zhang, R. Yu, Y. X. Su, Y. Song, M. Y. Wang, G. T. Tan, T. Egami, J. A. Fernandez-Baca, E. Faulhaber, Q. Si, and P. C. Dai, Phys. Rev. Lett. **111**, 207002 (2013).

[16] C. L. Zhang *et al.*, Phys. Rev. B **90**, 140502(R) (2014).

[17] D. J. Scalapino, Rev. Mod. Phys. **84**, 1383 (2012).

[18] P. J. Hirschfeld, M. M. Korshunov, and I. I. Mazin, Rep. Prog. Phys. **74**, 124508 (2011).

[19] A. Chubukov, Annu. Rev. Condens. Matter Phys. **3**, 57 (2012).

[20] M. M. Korshunov and I. Eremin, Phys. Rev. B **78**, 140509(R) (2008).

[21] T. A. Maier, S. Graser, D. J. Scalapino, and P. Hirschfeld, Phys. Rev. B **79**, 134520 (2009).

[22] T. A. Maier, S. Graser, D. J. Scalapino, and P. J. Hirschfeld, Phys. Rev. B **79**, 224510 (2009).

[23] P. Goswami, P. Nikolic, and Q. Si, Europhys. Lett. **91**, 37006 (2010).

[24] G. T. Tan, P. Zheng, X. C. Wang, Y. C. Chen, X. T. Zhang, J. L. Luo, T. Netherton, Y. Song, P. C. Dai, C. L. Zhang, and S. L. Li, Phys. Rev. B **87**, 144512 (2013).

[25] P. Cai, X. D. Zhou, W. Ruan, A. F. Wang, X. H. Chen, D. H. Lee, and Y. Y. Wang, Nat. Commun. **4**, 1596 (2013).

[26] S. Oh, A. M. Mounce, J. A. Lee, W. P. Halperin, C. L. Zhang, S. Carr, P. Dai, A. P. Reyes, and P. L. Kuhn, Phys. Rev. B **88**, 134518 (2013).

[27] L. Ma, J. Dai, P. S. Wang, X. R. Lu, Y. Song, C. L. Zhang, G. T. Tan, P. C. Dai, D. Hu, S. L. Li, B. Normand, and W. Q. Yu, Phys. Rev. B **90**, 144502 (2014).

[28] C. Bernhard, C. N. Wang, L. Nuccio, L. Schulz, O. Zaharko, J. Larsen, C. Aristizabal, M. Willis, A. J. Drew, G. D. Varma, T. Wolf, and C. Niedermayer, Phys. Rev. B **86**, 184509 (2012).

[29] X. Y. Lu, D. W. Tam, C. L. Zhang, H. Q. Luo, M. Wang, R. Zhang, L. W. Harriger, T. Keller, B. Keimer, L.-P. Regnault, T. A. Maier, and P. C. Dai, Phys. Rev. B **90**, 024509 (2014).

[30] Q. Q. Ge, Z. R. Ye, M. Xu, Y. Zhang, J. Jiang, B. P. Xie, Y. Song, C. L. Zhang, P. C. Dai, and D. L. Feng, Phys. Rev. X **3**, 011020 (2013).

[31] R. Yu, J. X. Zhu, and Q. Si, Phys. Rev. B **89**, 024509 (2014).

[32] Z.-H. Liu, P. Richard, K. Nakayama, G.-F. Chen, S. Dong, J.-B. He, D.-M. Wang, T.-L. Xia, K. Umezawa, T. Kawahara, S. Souma, T. Sato, T. Takahashi, T. Qian, Y. B. Huang, N. Xu, Y. B. Shi, H. Ding, and S.-C. Wang, Phys. Rev. B **84**, 064519 (2011).

[33] S. Thirupathaiah, D. V. Evtushinsky, J. Maletz, V. B. Zabolotnyy, A. A. Kordyuk, T. K. Kim, S. Wurmehl, M. Roslova, I. Morozov, B. Büchner, and S. V. Borisenko, Phys. Rev. B **86**, 214508 (2012).

[34] C. L. Zhang *et al.*, Phys. Rev. B **88**, 064504 (2013).

[35] J. Knolle, I. Eremin, J. Schmalian, and R. Moessner, Phys. Rev. B **84**, 180510(R) (2011).

[36] W. C. Lv, A. Moreo, and E. Dagotto, Phys. Rev. B **89**, 104510 (2014).

[37] Y. Song, S. V. Carr, X. Y. Lu, C. L. Zhang, Z. C. Sims, N. F. Luttrell, S. Chi, Y. Zhao, J. W. Lynn, and P. C. Dai, Phys. Rev. B **87**, 184511 (2013).

[38] J. W. Lynn, Y. Chen, S. Chang, Y. Zhao, S. Chi, W. Ratcliff, B. G. Ueland, and R. W. Erwin, J. Res. NIST **117**, 61 (2012).

[39] S. L. Li, C. de la Cruz, Q. Huang, G. F. Chen, T.-L. Xia, J. L. Luo, N. L. Wang, and P. C. Dai, Phys. Rev. B **80**, 020504(R) (2009).

[40] X. Y. Lu, J. T. Park, R. Zhang, H. Q. Luo, A. H. Nevidomskyy, Q. Si, and P. C. Dai, Science **345**, 657 (2014).